Published in final edited form as:
Integr Biol (Camb). 2010 January ; 2(1): 58–64. doi:10.1039/b918440f.

Study of Na^+/H^+ exchange-mediated pH_i regulations in neuronal soma and neurites in compartmentalized microfluidic devices

Lucas Vitzthum[1,4,*], **Xinzhi Chen**[1,2,*], **Douglas B. Kintner**[1], **Yu Huang**[4], **Shing-Yan Chiu**[3], **Justin Williams**[4], and **Dandan Sun**[1,2]

[1]Dept. of Neurological Surgery, Univ. of Wisconsin Madison, WI 53705

[2]Dept. of Neuroscience Training Program, Univ. of Wisconsin Madison, WI 53705

[3]Dept. of Physiology, School of Medicine and Public Health, Waisman Center; Univ. of Wisconsin Madison, WI 53705

[4]Dept. of Biomedical Engineering; Univ. of Wisconsin Madison, WI 53705

Abstract

Regulation of intracellular pH (pH_i) in neurons is crucial to maintain their physiological function. In the current study, newly-developed polydimethylsiloxane (PDMS) microfluidic devices were used to independently investigate pH_i regulation in neuronal soma and neurites. Embryonic cortical neurons were cultured in PDMS microfluidic devices with soma growing in one chamber (seeded) and neurites extending through a set of perpendicular microchannels into the opposite parallel chamber (non-seeded). Neurons in the microchambers were characterized by the vital dye calcein-red, polarized mitochondria, neuronal specific β-tubulin (type-III), axonal Tau-1 protein, dendritic microtubule associated protein (MAP-2), and Na^+/H^+ exchanger isoform 1 (NHE-1). Neurites exhibited higher resting pH_i than soma (7.16 ± 0.09 vs. 6.90 ± 0.15). The neurites had a proton extrusion rate 3.7-fold faster than in soma following NH_4Cl prepulse-mediated acidification ($p < 0.05$). The difference in the pH_i regulation rates between neurites and soma can be accounted for by the larger surface area to volume ratio in the neurites. Interestingly, inhibition of NHE-1 activity pharmacologically blocked the pH_i regulation in soma and in neurites by ~ 70% ($p < 0.05$). Taken together, our study demonstrated that the microfluidic devices provide a useful tool to study neuronal pH_i regulation in soma and their neurites. We conclude that NHE-1 plays an important role in regulation of pH_i in both compartments.

Keywords

pH_i regulation; somata; dendrites; Na^+/H^+ exchanger; dendritic microtubule associated protein

INTRODUCTION

Intracellular pH (pH_i) can rapidly fluctuate in response to neuronal activity or pathological insults.[1] The tight regulation of intracellular and extracellular pH (pH_i and pH_o) homeostasis is required for neuronal function in the central nervous system (CNS). Changes in pH_i (even in a small range) affect the functions of multiple enzymes, ion channels, and other

Address correspondence to: Dandan Sun, M.D., Ph.D., Department of Neurological Surgery, University of Wisconsin Medical School, T513 Waisman Center, 1500 Highland Ave., Madison, WI 53705, Phone: (608) 263-4060, FAX: (608) 263-1409, sun@neurosurg.wisc.edu.
*These Authors Contributed Equally

macromolecules, thus affecting synaptic transmission, neuronal excitability, and gap junction conductance.[2–4] pH_i may function as an important variable in regulating neurotransmitter release. [5,6] The Na^+/H^+ exchangers (NHEs) are acid extrusion proteins which catalyze the electrochemically neutral exchange of Na^+ into the cell and H^+ out of the cell at a ratio of 1 Na^+: 1 H^+.[7] NHEs are extremely sensitive to pH_i and characterized by the fact that they are allosterically activated by cytosolic H^+, thereby promoting the rapid extrusion of acid when pH_i drops below a threshold level. [7,8] The Na^+/H^+ exchanger 1 (NHE-1) is the most ubiquitous isoform in the CNS [9] and plays an important role in regulation of pH_i in neurons and astrocytes. [8] NHE1 activity is stimulated by growth factors, peptide hormones[7], and pathological stimuli such as ischemic-hypoxia.[10,11]

We recently reported that pH_i regulation rates in the dendrites of cultured cortical neurons grown in culture dishes were 330% higher then in the soma primarily because of the higher surface area to volume rates in dendrites.[12] The traditional *in vitro* neuronal culture models using culture dishes can not be used to independently investigate differential pH_i regulation between soma and neurites. Thus, the *in vitro* compartmentalized neuronal culture models make this type of study possible. Campenot first introduced a compartmentalized fluidic neuronal culture using a device consisting of a Teflon® divider attached to a collagen coated Petri dish with silicon grease.13 These devices required great skill to assemble and were difficult for imaging and prone to leakage.[13] Recently, compartmentalized microfluidic devices have been made of biologically inert polydimethylsiloxane (PDMS) that allows neurites to grow into isolated fluidic environments.14 Such devices have been applied in studying of axonal injury and regeneration14, axon myelination15, and drug-induced axonal degeneration. 16 Moreover, the enclosed microfluidic system provides a more physiologically relevant micro-environment (larger cell surface area to culture medium ratios) than culture dishes.[17]

In the current study, we developed an enclosed, compartmentalized microfluidic platform to examine the differential pH_i regulation in neuronal soma and neurites. Cultured cortical neurons were characterized with vital dyes (calcein and Mitotracker) and immunocytochemistry staining. Resting pH_i levels and pH_i recovery rates were measured in neurites and soma independently. Our report suggests that NHE-1 plays an important role in neuronal pH_i regulation.

METHODS

Materials

Hanks balanced salt solution (HBSS) was from Mediatech Cellgro (Manassas, VA). Neurobasal medium, B-27 supplement, MitoTracker green, calcein-AM, SYTO 60, and BCECF-AM were from Invitrogen (Carlsbad, CA). HOE 642 was a kind gift from Aventis Pharma (Frankfurt, Germany). Nigericin and antibody for MAP-2 were purchased from Sigma (St. Louis, MO). Antibody for β-tubulin (type-III) was obtained from Promega (Madison, WI). Tau-1 antibody was obtained from Santa Cruz Biotechnology (Santa Cruz, CA). SU-8 2 and SU-8 2001 were purchased from Microchem (Newton, MA). Polydimethylsiloxane (PDMS) was purchased from Dow Corning (Sylgard 184, Midland, MI). G116 antibody was a kind gift from Dr. Leong L. Ng (Leicester, UK).

Fabrication of microfluidic device

The microfluidic devices were fabricated in PDMS using rapid prototyping and soft lithography.[18,19] The layout of the microfluidic devices is shown in Figure 1 A, which consisted of two parallel chambers (seeded and non-seeded, 0.4 mm wide × 16 mm long × 0.25 mm tall) and bridging microchannels (30 μm wide × 200 – 300 μm long × 3 μm tall). Two corresponding transparency masks were printed from an EPS file using a 6,000 dpi high-resolution printer

(Imagesetter Inc, Madison, WI). A dual-layered negative master was fabricated by patterning dual layers of the epoxy based photoresist SU-8 2 (one for the microchannels, one for the two chambers). The photoresist was spun on a silicon wafer at a spin speed of 1500 rpm for 40 sec to obtain an approximate height of 3 μm for the bridging microchannels. The photoresist SU-8 2100 was subsequently spun on the silicon wafer (1100 rpm for 40 sec, 0.25mm in height) to create the non-seeded and seeded chambers. Both mask layers were carefully aligned with a technique (error < 15 μm) as described recently.[20] Microfluidic devices were fabricated by molding PDMS against this negative master. After degassing, PDMS (10:1 ratio base to catalyst) and the wafer were heated in a hot plate at 120 °C for 30 min. Inlets and outlets for fluid exchange in each chamber (1/8 inch in diameter) were made in the resulting PDMS microdevice (1.5 mm thick). PDMS microdevices were placed on poly-D-lysine coated glass coverslips (22 × 22 mm) and sterilized by autoclave.

Primary neuron culture in microfluidic devices

Pure cortical neurons from mouse embryonic day 14–16 fetuses (E14-16) were prepared as described before.[21] In brief, the cortices were removed from E14-16 fetuses and treated with 0.5 mg/ml trypsin at 37°C for 25 min. The cells were centrifuged at 300 g for 4 min at 4°C. The cell pellet was diluted in B-27 supplemented Neurobasal medium (2 %) containing 0.5 mM L-glutamine and penicillin/streptomycin (100 units/ml and 0.1 mg/ml, respectively). As shown in Figure 1 A, the cells were seeded at a density of 500 cells/mm^2 in the seeded chamber by passive pumping[22]. Briefly, the seeded chamber was rinsed with Neurobasal medium by adding a drop (~20 μL) into the inlet and aspirating from the outlet (Figure 1 A). The non-seeded chamber was rinsed with the fresh medium similarly. Cells were seeded via passive pumping by adding ~ 10 μL of a 2×10^6/ml cell suspension to the inlet which then flowed into the seeded chamber due to a low surface tension created by the large drop of medium placed on the outlet. The microfluidic devices were placed in an incubator at 37°C (model 3130, Thermo Forma, Waltham, MA) with 5% CO_2 and atmospheric air. A blank PDMS piece (~ 0.5 mm thick) was placed over the chamber ports on day 2 in vitro (DIV 2) to prevent medium evaporation. DIV 8–11 cultures were used in the study.

Measurement of pH_i after NH_4^+/NH_3 pre-pulse

Neuronal cultures in the microfluidic device were incubated with 10 μM BCECF-AM in $HC0_3^-$-free HEPES buffered medium at 37°C for 30 min. Microfluidic devices were then mounted on a temperature controlled (37°C) imaging chamber (Warner Instruments, Hamden, CT). The chamber was placed on the stage of the TE 300 inverted epifluorescence microscope and visualized with a 40× oil-immersion objective. The cells were excited every 1–20 s at 490 and 440 nm, and the emission fluorescence at 535 nm recorded. Images were collected using a Princeton Instruments MicroMax CCD camera. Regions of interest were drawn either in the cytosol of 20 cells (seeded side) or on neurites (non-seeded side) and analyzed with MetaFluor image-processing software. At the end of each experiment, the ratio of the background-corrected fluorescence emissions (F490/F440) was calibrated using the high K^+/nigericin technique.[23] In this study, the inherent error in determining pH_i with the BCECF method is ~ 1.5% (supplemental Figure 1). Microchamber fluid replacement in these experiments was accomplished by placing a drop of solution with a 25 μl Hamilton syringe on the inlet of one microchamber and quickly drawing the fluid through the outlet with the corner of a Kimwipe®.

For the pre-pulse treatment, either soma (the seeded-chamber) or neurites (non-seeded chambers) were subjected to an acid load by transient application (5 min) of 30 mM NH_4^+/NH_3 solution.[24] NH_4^+/NH_3 solutions were prepared by replacing 30 mM NaCl in the HCO_3^--free HEPES-buffered solution with an equimolar concentration of NH_4Cl. Application of NH_4^+/NH_3 solution caused pH_i to rise as NH_3 gas diffused quickly into the cell and combined with H^+ to form NH_4^+. After 5 min, the NH_4^+/NH_3 solution was replaced with HCO_3^--free

HEPES-buffered solution, causing NH_3 to leave the cell and trapping H^+ in the cell. This is the classic method of placing an artificial acid load on cells to characterize pH_i regulation.[25] Interestingly, we observed that the pre-pulse treatment applied to one microchamber (soma or neurites) did not cause either alkalization or acidification in the opposite chamber (data not shown). This suggests that we are able to investigate pH_i regulation in these compartments (ie. between soma and neurites), separately. Before returning cells to normal HCO_3^--free HEPES-buffered solution to acidify the cells, the image acquisition interval rates was increased to 1 HZ in order to monitor pH_i recovery. pH_i recovery rate was determined from the slope of a fitted linear regression fit to the initial linear portion of the trace after NH_4^+/NH_3 application (5–30 sec).[24]

Resting pH_i was averaged from the first ~2 min incubation of cells with HCO_3^-- HEPES-buffered normal solution before the pre-pulse was performed. In the experiments with specific NHE-1 inhibitor HOE 642, either soma or neurites were incubated with HOE 642 (1 μM) for 10 min prior to and then throughout the NH_4^+/NH_3 pre-pulse.

Live cell imaging

To determine surface area to volume ratios in pure neuron cultures growing in microchamber devices, neurons were loaded with 0.5 μM calcein-AM green (a vital dye) and 5 μM SYTO 60 (nucleus dye) for 30 min at 37°C. The coverslips were then placed in the perfusion chamber on the stage of a Leica DMIRE2 confocal microscope and visualized with a 100× 1.4 NA apochrome oil-immersion objective. An ~15 μm (neurites) to 30 (somata) μm thick image stack (150–250 slices at 512 by 512 pixels) was collected sequentially (ex. 488 nm argon laser line, em. 500–545 nm and ex. 543 HeNe laser, em 544–677) and imported into ImageJ (Version 1.41, NIH). A cellular region (somata, nucleus, or process) was defined and the surface area was calculated by summing the product of the region perimeter by the distance between each image section (0.12 μm). The volume of the region was calculated with the region area and intra-section distance. The somata volume was corrected by subtracting the calculated volume for the nucleus volume. In other experiments, neurons in microchambers were further characterized by duel-labeling with 0.5 μM calcein-AM red and 0.2 μM MitoTracker green, a mitochondrial-selective fluorescent dye, for 30 min. Calcien-AM and Mitotracker images were sequentially captured with a Leica DMIRE2 confocal microscope using a 20× objective and 543 nm HeNe and a 488 nm argon lasers respectively.

Immunofluorescence staining

PDMS microfluidic devices were removed from the glass coverslips and the cells on the coverslips were gently rinsed with PBS (pH 7.4) and fixed with 4% paraformaldehyde in PBS.[24] After rinsing, cells were incubated with blocking solution (10% normal goat serum, 0.4% Triton X-100, and 1% bovine serum albumin in PBS) for 1 h at room temperature. Cells were incubated for 1 h at 37°C with polyclonal G116 NHE-1 antibody (1:50), mouse monoclonal MAP-2 antibody (1:200), monoclonal β tubulin (type-III) antibody (1: 200) or rabbit polycolonal Tau-1 antibody (1:100). After rinsing in PBS, cells were incubated with goat anti-mouse Alexa 488-conjugated IgG (1:100; Invitrogen), goat anti-rabbit Alexa 546 conjugated IgG (1:100; Invitrogen, for confocal microscopy) or goat anti-rabbit Alexa 594 conjugated IgG (1:100; Invitrogen, for epifluorescence microscopy) for 1 h at 37°C. 1 μg/mL To-pro-3 iodide was used to stain nuclei for confocal image collection. Fluorescence images were captured by the Nikon TE 300 inverted epifluorescence microscope (20×) using a Princeton Instruments MicroMax CCD camera and MetaMorph image-processing software. Negative controls were incubated with secondary antibodies only. Identical digital imaging acquisition parameters were used in both negative control and experimental images. Images of Tau-1 (20×) were captured with a Leica DMIRE2 confocal microscope using an 543 nm HeNe laser for Alexa Fluor 546, and a 640 nm GreNe laser for To-pro-3 iodide signals.

Statistics

Paired Student's t-test was used for comparisons between groups and analysis of variance with the Bonferroni post-test for multiple comparisons (SigmaStat, Systat Software, Point Richmond, CA). When comparison groups did not have normal distribution or equal variance, a Mann-Whitney Rank Sum Test was used. A P-value of < 0.05 was considered as significantly different.

RESULTS

Neuronal growth and differentiation in the microfluidic system

Neurons were grown in the PDMS microfluidic system as described in Methods. DIV 8–11 cultures were loaded with the vital dye calcein red and MitoTracker green (Figure 1 B). Both soma and neurites retained calcein-red, indicating intact plasma membrane integrity of neurons in the culture (Figure 1 B, a). Figure 1 B (a, b) also illustrate that the neurites grew across the bridge-channels and protruded into the non-seeded chamber. Concurrently, neuronal cultures were stained with the mitochondrial dye MitoTracker-green, which reacts with thiol groups of proteins and forms conjugates in the mitochondria, thus labeling mitochondria independent of their membrane potential. As shown in Figure 1 B (**c, d, arrows**), punctate MitoTracker-green signals were detected in soma and neurites. Interestingly, a high level of mitochondria was distributed in neurites in the non-seeded chamber (punctuate, rod-shape individual mitochondria in **d, f**). In contrast, Mitotracker-green signals were less evident in the neurites in the bridging channels, suggesting that MitoTracker green does not diffuse quickly within the intracellular space or through the bridging channels (Figure 1 B, c). An overlay of the calcein red and MitoTracker-green images revealed that the distal neurites expressed less calcein red (Figure 1 C). Taken together, these data illustrate that cortical neurons (in the seeded chamber) were able to grow and extend their neurites through the micro-bridging channels into the non-seeded chamber. Mitochondria appear to be enriched in the distal neurites in a similar manner as *in vivo*.

Characterization of neurons in microfluidic devices

Neurons cultured in the PDMS microfluidic devices were further characterized with immunofluorescence staining assays. First, expression of three neuronal marker proteins [β-Tubulin (type-III), Tau-1 and MAP-2] in the cultures was examined. As shown in Figure 2 A, β-Tubulin was abundantly expressed in neuronal soma and throughout the neurites. Moreover, dendritic marker protein MAP-2 was expressed in soma and dendritic neurites in the bridging channels and non-seeded chamber (Figure 2 B). In one occasion, small immature neurons migrated through the bridging channel and grew in the non-seeded chamber (**arrow**, Figure 2 B). In Figure 2 C, D, the axonal marker protein Tau-1 was expressed in the neurites growing into the non-seeded chamber, but with less immunointensity in neuronal soma (in the seeded-chamber) or in the neurites of the bridging channels. Negative control studies for these proteins were conducted by omitting the primary antibodies and illustrated no fluorescence signals (insets of Figure 2 A, B, C). These findings demonstrate that cortical neurons grow in the microfluidic devices with neurites (both axons and dendrites) extruding into the non-seeded chambers.

Next, we evaluated expression of an important pH_i regulatory protein NHE-1. As shown in Figure 2 E, F, NHE-1 was present in soma of the seeded-chamber and neurites in the non-seeded chambers. Negative control studies were shown in **insets of** Figure 2 E, F. No or low fluorescence signals in these controls were detected under the same data acquisition settings.

Regulation of pH_i in soma and neurites

We then independently determined pH_i regulatory responses in soma of the seeded chambers and neurites in the non-seeded chambers. pH_i recovery rate was measured following the NH_3/NH_4^+ prepulse-induced acidification. In the absence of HCO_3^-, pH_i regulation largely reflects NHE-mediated H^+ efflux.[26] As shown in Figure 3 A, when neuronal somata in the seeded chamber was exposed to 30 mM NH_3/NH_4^+, pH_i rose rapidly as NH_3 diffused into the cell and combined with H^+ to form NH_4^+ (**a–b**) and then declined slowly (**b–c**). Removal of the NH_3/NH_4^+Cl solution from the seeded chamber caused somata pH_i to decrease because the newly formed NH_4 rapidly left cells as NH_3, trapping H^+ inside of cells (**c–d**). Neurons were able to quickly restore somata pH_i at a rate of 1.25 ± 0.29 pH units/min < 3 min and returned to their basal levels (6.90 ± 0.15 pH). In some cases, there was an alkaline overshoot (Figure 3 A). In the presence of the potent NHE-1 inhibitor HOE 642 (1 μM), somata pH_i recovery rate was significantly reduced (0.35 ± 0.13 pH units/min, $p < 0.05$, Figure 3 A, C) and the alkaline overshoot was blocked.

After NH_3/NH_4^+ prepulse-induced acidification, the neurites exhibited much faster pH_i recovery kinetics (4.59 ± 0.86 pH units/min, Figure 3 B, C). Inhibition of NHE-1 with HOE 642 reduced the recovery rate to 1.47 ± 0.14 pH units/min in neurites ($p < 0.05$, Figure 3 B, C). Moreover, a more alkaline basal pH_i (7.16± 0.09) was detected in the neurites than in soma (Figure 3 D).

Determination of surface area and volume (A/V) ratio in soma and neurites

The apparent higher pH_i recovery rates in the neurites could result from significantly larger A/V ratios in the neurites. A/V ratios were determined in somata (**arrow**) and neurites (**arrow-head**) as illustrated in Figure 4 A, B. Figure 4 C shows that the A/V ratio in the neurites is 2.8 times higher than that of soma. Interestingly, the A/V ratios of soma and neurites were higher in the microfluidic devices than in cells cultured on coverslips in traditional plastic 35 mm culture dishes (Figure 4 C).[12] Although digital 3-D reconstruction from 2-D data sets will tend to underestimate surface areas by smoothing the images, this estimate of A/V ratios served as approximation for correcting pH_i regulation rates.

Consequently, we corrected the pH_i recovery rate for the A/V ratios in soma and neurites (Table-1). After the correction, the differences in H^+ extrusion rates in the two regions were abolished. Once the soma pH_i recovery rates were corrected for A/V ratio they were comparable to the corrected rates that were observed in neurons in 35 mm culture dishes (0.30 ± 0.07 vs. 0.30 ± 0.01 pH units/min respectively) [12]. However, the A/V-corrected pH_i recovery rates in neurites grown in microfluidic devices (0.40 ± 0.08 pH units/min) remained significantly higher than in neurites grown in the culture dishes (0.19 ± 0.04, $p < 0.05$).[12]

Discussion

Characterization of cultured neurons in microfluidic devices

Our results showed viable neuronal growth in the seeded-chamber with neurites expanding through the bridging channels and into the non-seeded chamber. In most cases, the calcein signals were colocalized with the MitoTracker signals, indicating the intact integrity of plasma membrane and mitochondria. Damaged neurons would not retain either dye. Taken together, these results demonstrate that we have developed a viable compartmentalized microfluidic system for culturing neurons.

Microfluidic devices with micro-bridging channels lengths greater than 200 μm exhibit almost exclusively axonal growth and a few dendrites in the non-seeded chambers at DIV 14.[14] In contrast, both dendrites and axons extend through 150 μm long bridging channels at DIV 14.

[14] In our study, we used 200–300 μm long bridging channels. We observed abundant expression of neuronal specific β-III tubulin and dendritic protein MAP-2 in both soma and neurites, while the neurites in the non-seeded chambers of DIV 8–11 neuron cultures exhibited abundant expression of the axonal marker protein Tau-1. Because both axons and dendrites were present in the non-seeded chambers in the current study, we are unable to differentiate between the two with regard to pH_i measurement in the non-seeded chamber. Therefore, in the non-seeded channels we referred them as neurites.

There was a noticeable lack of MitoTracker-labeled mitochondria within the micro-bridging channels. This most likely resulted from restricted access of the MitoTracker dye to the mitochondria within the micro-bridging channels. To reach mitochondria within the micro-bridging channel, a dye must either enter the bridging-channel and then be taken up by the cell or enter the cell and then be transported through the cytoplasm to reach mitochondria in the neurites of the bridging-channel. Movement of the dye depends on molecular diffusion which is driven by concentration gradients of the dye. Upon entering the cell, MitoTracker is concentrated in nearby mitochondria where it covalently binds to proteins and would be unavailable to reach mitochondria located further away. However, we can not rule out that the low density of mitochondria in the micro-bridging channel determined with MitoTracker staining could be the result of its shallow height (3 μm) which would limit mitochondrial congregation.

Differential regulation of pH_i in soma vs. neurites

The high fluidic resistance of the micro-bridging channels produces a small but sustained flow between the seeded and non-seeded chambers that counteracts diffusion. The fluidic isolation between the two chambers can last for 20 h owing to the high fluidic resistance of the micro-bridging channels.[14] Thus, the fluidic resistance allows us to measure pH_i regulation in soma and neurites independently. We found that neurites exhibited more alkaline resting pH_i than in soma (7.16 ± 0.09 vs. 6.90 ± 0.15). The neurites were able to change $[H^+]$ 3.7-fold faster than soma following NH_4Cl prepulse-mediated acidification ($p < 0.05$). Interestingly, inhibition of NHE-1 activity pharmacologically blocked the pH_i regulation in soma and neurites by ~ 70% ($p < 0.05$). Moreover, the presence of NHE-1 isoform protein was detected in both neuronal soma and neurites, supporting its role in the pH_i regulation. Investigating the mechanisms involved in pH_i regulation in soma and dendrites is important to understand how the cell counteracts the robust intracellular acidification that occurs during synchronous neural activity.[27] In addition, we have recently reported that the selective vulnerability of dendrites to ischemic insults may involve overstimulation of NHE-1 activity.[12]

The more alkaline basal pH_i observed in neurites suggests that increased NHE1 function could have significant metabolic consequences under physiological and pathological conditions. For example, NHEs are major intraterminal pH_i regulators on GABAergic presynaptic nerve terminals and play an important role in the neuronal excitability by increasing inhibitory tones.[1] It is recently reported that NHE1 accumulates at the leading edge of neurites where it alkalizes growth cones and regulates membrane protrusion and directional motility.[28] On the other hand, NADPH oxidase is inhibited by low pH_i, thus, increased NHE1 activity could increase formation of reactive oxygen species and potentiate reactive oxidative damage in neurites.[29]

We found that the A/V ratio in the neurites is 2.8 times higher than that of soma grown in microfluidic devices. In addition, the A/V ratios of soma and neurites were higher in the microfluidic devices than in the traditional plastic plates. The reason for the difference in A/V ratios between neurons grown in culture dishes vs. microfluidic devices is not clear. It could be because of the difference in "effective culture volume" (ECV) between the two.[30] The ECV is a measure of the cell's control over its local environments and a function of the magnitude of mass transport along each axis, the effects of diffusion and convection, and the degree of

protein adsorption to surfaces. 30 I*n vivo*, extracellular molecules such as secreted growth factors have a crucial role in determining cell shape.[31] These signals would be lost through dilution in culture dishes. We speculate that the neuronal cell shape and A/V ratios in microscale cultures result from extracellular microenvironments which are not present in culture dishes.

In addition, the significantly higher NHE-1 activity in the neurites in microfluidic devices than in the culture dishes could also result from the density of NHE-1 expression or post-translational regulation (phosphorylation state of the protein). Further investigation is needed to define the influence of the culture microenvironment on pH_i regulation through NHE-1.

In summary, we reported here that dissociated pure cortical neurons were cultured in the microfluidic devices with neurites grown across a 200–300 μm bridging-channels. The microfluidic devices allowed us to successfully examined pH_i in the two compartments independently. We detected that neurites exhibited more alkaline resting pH_i than in soma. The neurites had a pH_i regulation rate 3.7-fold faster than in soma following acidification. These findings suggest that the NHE1's role in maintaining alkaline resting pH_i in neurites may regulate function of NMDA receptor activity, voltage-gated Ca^{2+} channel, and synaptic vesicle-mediated exocytosis.

Supplementary Material

Refer to Web version on PubMed Central for supplementary material.

Acknowledgments

This work was supported in part by NIH grants R01NS38118 and R01NS048216 (D. Sun), and an AHA Established-Investigator award grant N0540154 (D. Sun); MS RG-4054-A-8 (S.Y. Chiu).

References

1. Jang IS, Brodwick MS, Wang ZM, Jeong HJ, Choi BJ, Akaike N. J. Neurochem 2006;99:1224–1236. [PubMed: 17018119]
2. Tombaugh GC. J. Neurophysiol 1998;80:1702–1712. [PubMed: 9772233]
3. Trudeau LE, Parpura V, Haydon PG. J. Neurophysiol 1999;81:2627–2635. [PubMed: 10368383]
4. Somjen, GG.; Tombaugh, GC. pH modulation of neuronal excitabiliity and central nervous system functions. In: Kaila, K.; Ransom, BR., editors. pH and Brain Function. New York: Wiley-Liss; 1998. p. 373-394.
5. Chesler M, Kaila K. Trends Neurosci 1992;15:396–402. [PubMed: 1279865]
6. Chesler M. Physiol Rev 2003;83:1183–1221. [PubMed: 14506304]
7. Orlowski J, Grinstein S. Pflugers Arch 2004;447:549–565. [PubMed: 12845533]
8. Kintner DB, Wang Y, Sun D. Front Biosci 2007;12:762–770. [PubMed: 17127336]
9. Ma E, Haddad GG. Neuroscience 1997;79:591–603. [PubMed: 9200742]
10. Luo J, Chen H, Kintner DB, Shull GE, Sun D. J. Neurosci 2005;25:11256–11268. [PubMed: 16339021]
11. Kintner DB, Look A, Shull GE, Sun D. Am. J. Physiol Cell Physiol 2005;289:C934–C945. [PubMed: 15901600]
12. Kintner DB, Chen X, Chiu SY, Baba A, Matsuda T, Cohen MS, Orlowski J, Taunton J, Sun D. J. Neurosci. 2009
13. Campenot RB. Proc. Natl. Acad. Sci. U. S. A 1977;74:4516–4519. [PubMed: 270699]
14. Taylor AM, Blurton-Jones M, Rhee SW, Cribbs DH, Cotman CW, Jeon NL. Nat. Methods 2005;2:599–605. [PubMed: 16094385]
15. Park J, Koito H, Li J, Han A. Biomed. Microdevices. 2009

16. Yang IH, Siddique R, Hosmane S, Thakor N, Hoke A. Exp. Neurol 2009;218:124–128. [PubMed: 19409381]
17. Pearce TM, Williams JC. Lab Chip 2007;7:30–40. [PubMed: 17180203]
18. Whitesides GM, Ostuni E, Takayama S, Jiang X, Ingber DE. Annu. Rev. Biomed. Eng 2001;3:335–373. [PubMed: 11447067]
19. O'Neill A, Soo Hoo J, Walker GM. Lab Chip: Chips and Tips. 2006
20. Yu, H.; Pope, R.; Williams, J. Conf. Proc. IEEE Eng Med. Biol. Soc; 2009.
21. Chen X, Kintner DB, Luo J, Baba A, Matsuda T, Sun D. J. Neurochem 2008;106:1563–1576. [PubMed: 18507737]
22. Walker GM, Beebe DJ. Lab Chip 2002;2:131–134. [PubMed: 15100822]
23. Boyarsky G, Ransom B, Schlue WR, Davis MB, Boron WF. Glia 1993;8:241–248. [PubMed: 8406681]
24. Kintner DB, Su G, Lenart B, Ballard AJ, Meyer JW, Ng LL, Shull GE, Sun D. Am. J. Physiol Cell Physiol 2004;287:C12–C21. [PubMed: 15013953]
25. Boron WF, De Weer P. J. Gen. Physiol 1976;67:91–112. [PubMed: 1460]
26. Luo J, Kintner DB, Shull GE, Sun D. J. Biol. Chem 2007;282:28274–28284. [PubMed: 17664275]
27. Makani S, Chesler M. J. Neurosci 2007;27:7438–7446. [PubMed: 17626204]
28. Sin WC, Moniz DM, Ozog MA, Tyler JE, Numata M, Church J. J. Neurosci 2009;29:8946–8959. [PubMed: 19605632]
29. Brennan AM, Suh SW, Won SJ, Narasimhan P, Kauppinen TM, Lee H, Edling Y, Chan PH, Swanson RA. Nat. Neurosci 2009;12:857–863. [PubMed: 19503084]
30. Walker GM, Zeringue HC, Beebe DJ. Lab Chip 2004;4:91–97. [PubMed: 15052346]
31. Bibel M, Barde YA. Genes Dev 2000;14:2919–2937. [PubMed: 11114882]

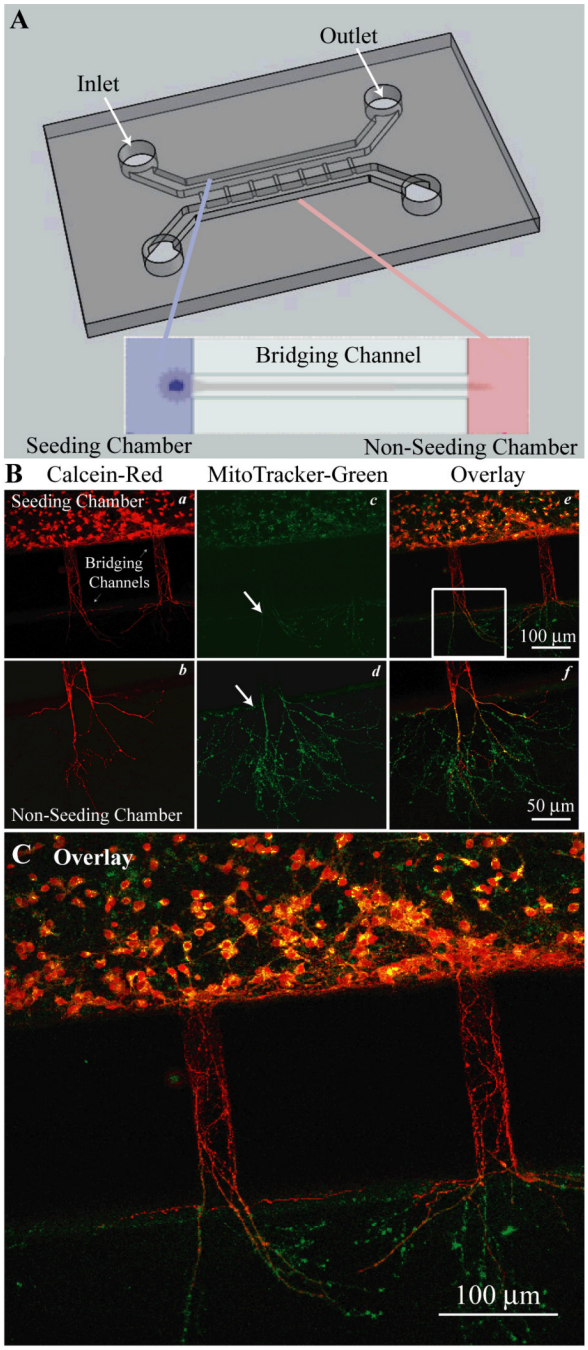

Figure 1. Cortical neuron cultures in PDMS microfluidic devices

A. Microfluidic devices were adhered to a poly-d-lysine (PDL) coated coverslips to create a water tight, gas permeable chamber. The devices had two larger parallel chambers (0.4 mm wide, 0.25 mm tall) labeled as the seeded and non-seeded chambers. Inlet and outlet ports through the PDMS were created for cell loading and media exchange. These chambers were connected by a series of 200–300 µm long micro-bridging channels (30 µm wide, 3–5 µm tall) that exclude neuronal soma, but through which neurites can extend. Expanded view shows neuronal soma in the seeded channel with processed extending through the bridging channel into the non-seeded channel. **B.** Neurons cultured in the microfluidic device were imaged with

calcein and MitoTracker dyes to access cell viability (***a–f***). **C.** An enlarged view of panel **B (f)** provides detailed information.

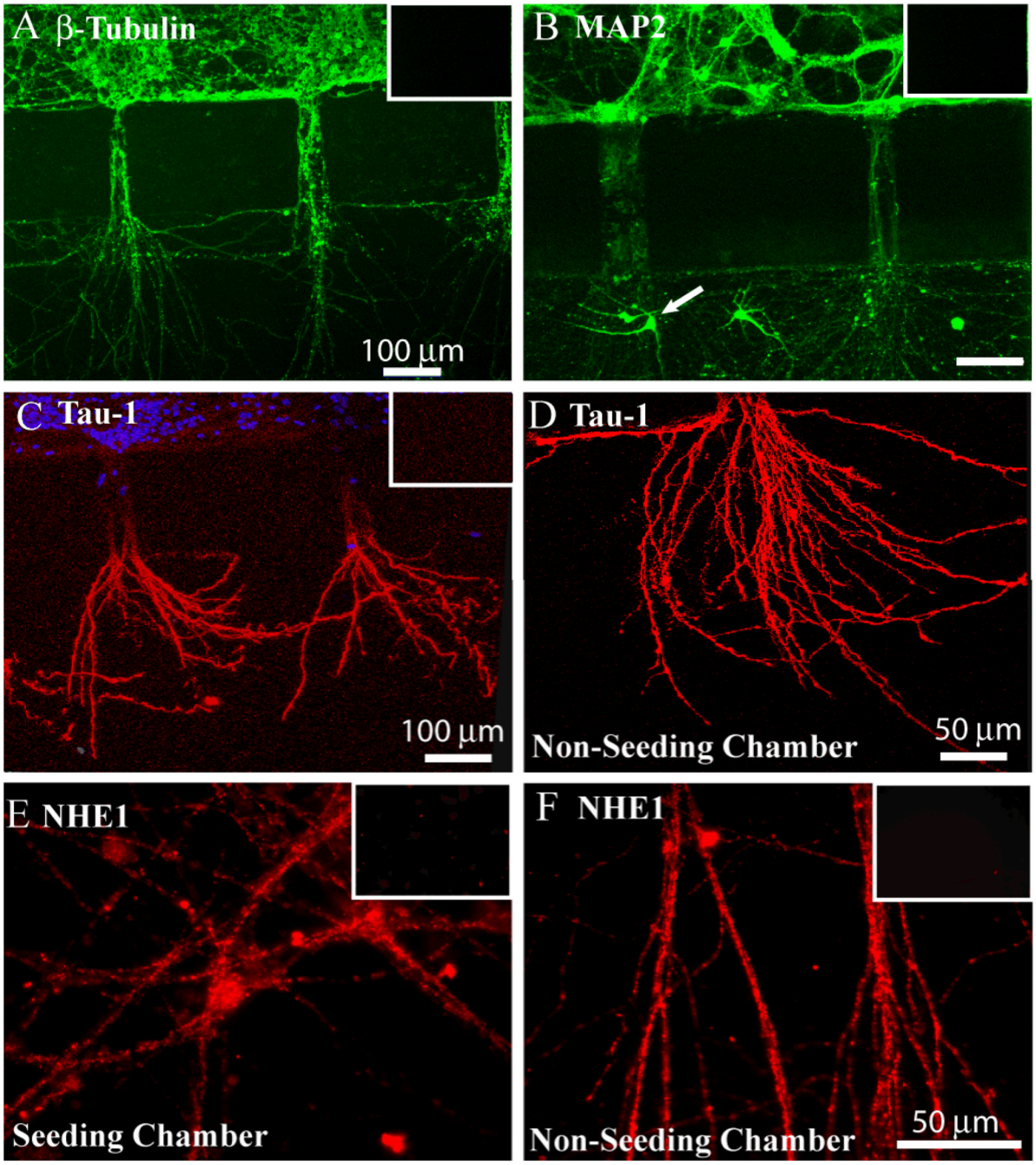

Figure 2. Characterization of neurons cultured in microfluidic devices

A. Neurons cultured in microfluidic device at DIV 8–11 stained for β-Tubulin. **B.** Neurons stained for MAP-2. **C, D.** Neurons stained for Tau-1 in microfluidic device **(C)** or in the non-seeded chamber **(D)**. **E, F.** Neurons stained for NHE-1 protein in the seeded- **(E)** and non-seeded chambers **(F)**. **Inset**, negative controls by omitting primary antibodies for β-Tubluin, MAP-2, Tau-1 or NHE-1 antibody. Scale bars = 100 µm in **A, B, C**. and = 50 µm in **D, E, F.**

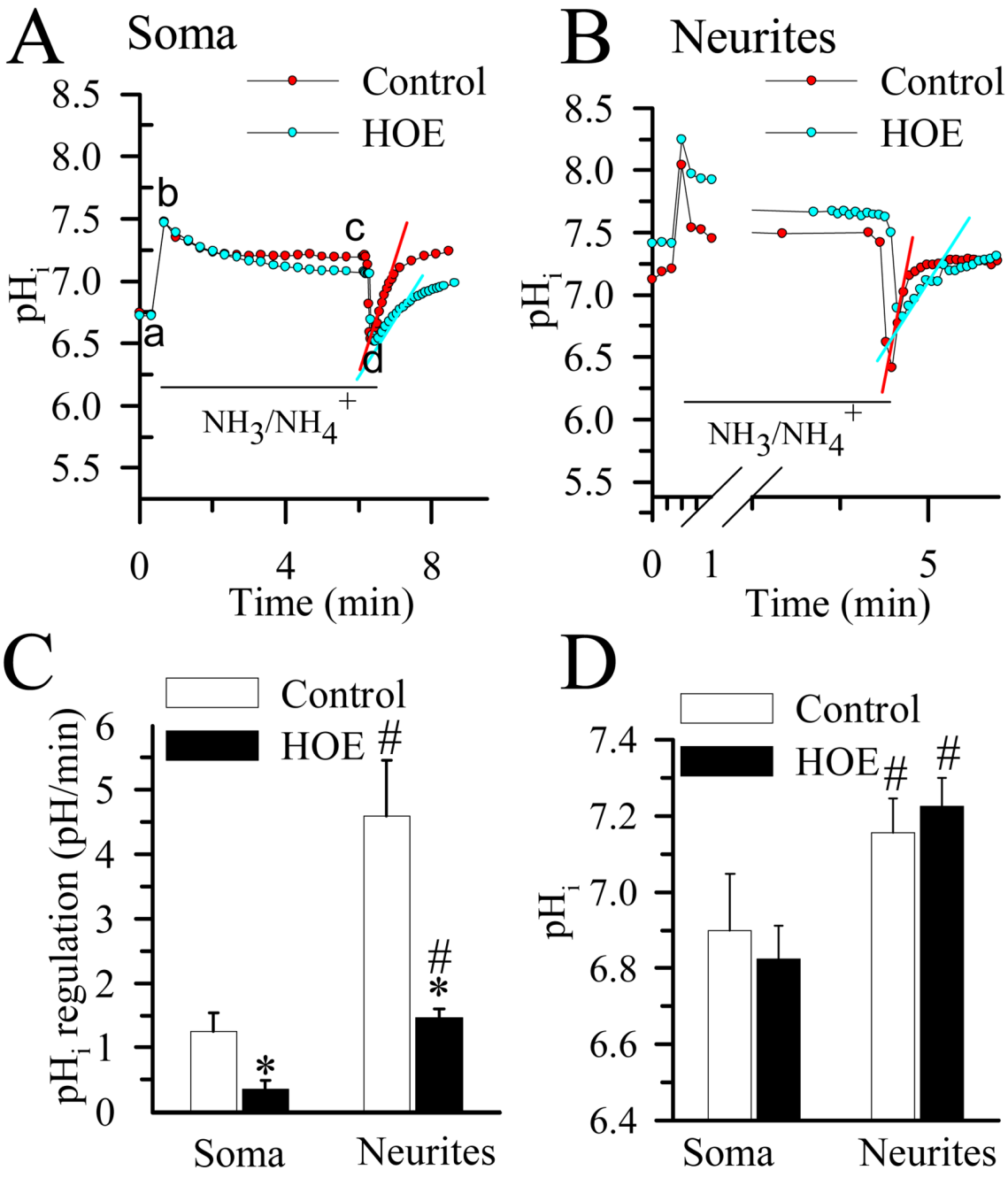

Figure 3. pH_i regulation in soma and neurites

pH_i recovery rates were determined in cortical neurons cultured in microfluidic devices at DIV 8–11. Representative tracings showing the pH_i changes in neuronal **A.** soma and **B.** neurites subjected to a prepulse acidification by exposure to 30 mM NH_4Cl for 5 min. Each point is the average of 20 regions of interest. pH_i recovery rates were determined by fitting a slope to the pH values over the linear portion of recovery following acidification. Red and blue slope lines are shown to illustrate the quantified rate of recovery. In some studies, 1 μM HOE 642 was present 10 min before and throughout the remaining NH_3/NH_4^+ prepulse experiments. **C.** Summary data of calculated pH_i recovery rates **D.** Summary data of resting pH_i values for

neuronal soma and neurites. Data are mean ± SEM. n = 5–6. * $p < 0.05$ vs. control; # $p < 0.05$ vs. soma.

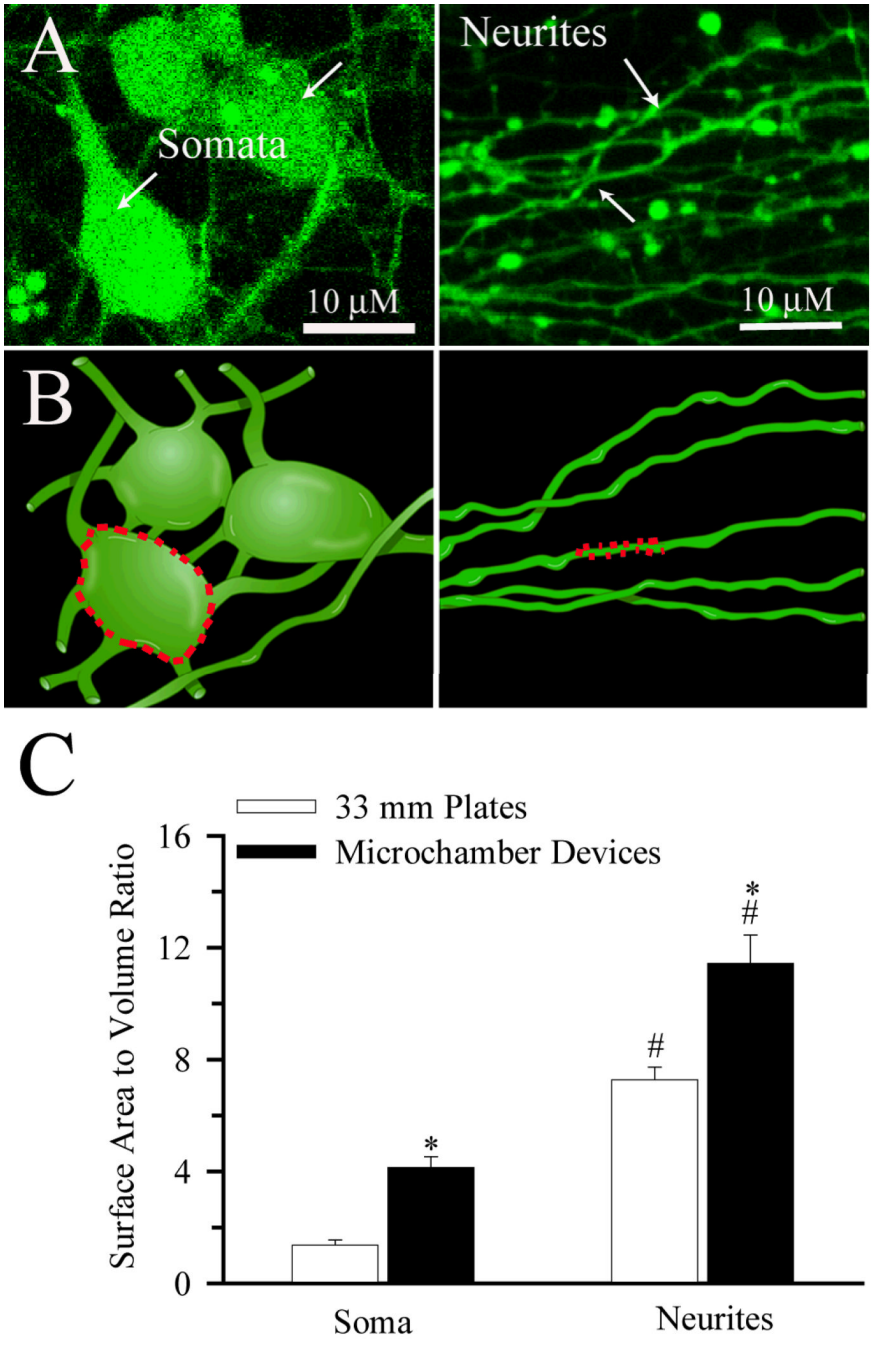

Figure 4. Topography and surface area to volume ratio of cultured neurons

A. A single 2D confocal image of neurons growing in the seeded-chamber loaded with 0.5 μM calcien-AM from a stack (30 μm) of 250 images (**Left Panel**). A single 2D confocal image of neurites as they emerged into the non-seeded chamber from a stack (15μm) of 150 images (**Right Panel**). **Arrows**: somata. **Arrowheads**: neurites **B**. Rendition of a 3D image produced from **A** to illustrate the surface area to volume ratio determination in soma and dendrites (**dotted lines**). **C**. Summary data of surface area to volume (A/V) ratios calculated in the soma of the seeded-chamber and neurites that extended into the non-seeded chamber. The A/V ratios in microdevices were further compared to ones collected in neurons grown on 35 mm plastic

plates[12]. Data are mean ± SEM. n = 8–14 cells. * $p < 0.05$ vs. 33 mm plastic plates. # $p < 0.05$ vs. soma.

Table 1

Surface Area to Volume (A/V) Ratio and corrected pH_i regulation in microfluidic devices

	A/V Ratio	pH_i Regulation Rate (pH units/min)	Corrected pH_i Regulation (pH units/min)
Soma	4.14 ± 0.39	1.25 ± 0.29	0.30 ± 0.07
Neurites	11.43 ± 1.02#	4.59 ± 0.86#	0.40 ± 0.08

Data are mean ± SEM.

# $p < 0.05$ vs. soma.